Kinetics and Catalysis, Vol. 45, No. 2, 2004, pp. 189–197. Translated from Kinetika i Kataliz, Vol. 45, No. 2, 2004, pp. 205–213.

CATALYTIC REACTION MECHANISMS

The Interaction of O_2, NO, and N_2O with Surface Defects of Dispersed Titanium Dioxide

A. A. Lisachenko, V. N. Kuznetsov, M. N. Zakharov, and R. V. Mikhailov

Institute of Physics, St. Petersburg State University, St. Petersburg, 198504 Russia

Received February 25, 2003

Abstract—A combined study of intrinsic structural defects in reduced TiO_2 was performed using mass spectrometry, optical diffuse-reflectance spectroscopy, and UV photoelectron spectroscopy (UPS). It was found that the reduction of TiO_2 resulted in the appearance of absorption in the region $0.50 \le h\nu \le 3.50$ eV ($400 \le \lambda \le 2500$ nm), which is formed by absorption due to free electrons (a continuum at $h\nu \le 1.50$ eV), local centers—Ti^{3+} ions (a band at 2.00 eV), and oxygen vacancies (bands at 1.17, 2.81, and 2.55 eV). The spectrum of induced occupied electronic states in the forbidden gap and the position of oxygen vacancy levels with respect to the Fermi level were determined by UPS. The absorption of reduced TiO_2 was stable on the sample to $T = 800$ K in a vacuum; however, it weakened in contact with O_2, NO, and N_2O molecules beginning at $T = 300$ K (surface sites) and $T \ge 400$ K (subsurface sites) as a result of filling oxygen vacancies with atomic oxygen in the course of dissociative adsorption. The adsorption complexes formed by the interaction of O_2, NO, and N_2O with defects were analyzed by temperature-programmed desorption. The distribution of sites over the energies of oxygen binding was found with the use of a nonuniform surface model, and specific oxygen adsorption species were revealed. It was found that the irradiation of TiO_2 activates the formation and decay of sites and results in the formation of specific O_2 and N_2O adsorption species.

INTRODUCTION

Titanium dioxide is one of the most commonly used photocatalysts for a wide variety of reactions [1–10]. The characteristic absorption edge of TiO_2 lies in the UV region ($\lambda \le 370$ nm); therefore, the sensitization of TiO_2 to longer wavelength radiation is a very topical problem [5, 6, 11, 12]. For this purpose, Ni, Fe, V, and Cr metal dopants are introduced to generate local electron centers in the forbidden gap, which are responsible for the absorption of visible light. However, these centers activate hole–electron recombination and thus decrease the activity of the photocatalyst in the region of intrinsic absorption [12].

The implantation of metal ions [5] made it possible to extend the range of effective radiation to $\lambda \ge 500$ nm. Anpo [5] believed that, in the second-generation photocatalysts developed, sensitization was due to changes in the local electronic structure of TiO_2 near the implanted ion. At the same time, the role of intrinsic TiO_2 defects in the photosensitization of reactions has not been adequately studied. It is well known [13] that defects such as oxygen vacancies and Ti^{3+} ions can appear in the course of redox reactions at the first step of the reaction (the reduction of TiO_2) and upon the exposure of a sample to UV light in a vacuum [1]. They can play the role of absorption centers in the visible region of the spectrum [11, 14, 15] and adsorption sites for reactants, reaction intermediates, and/or the final products of the reaction [16].

The aim of this work was to study the intrinsic local structural defects of reduced TiO_2; to analyze the conditions of their formation; to determine their optical, electronic, and structural characteristics; to examine adsorption complexes formed in the course of surface oxidation by O_2, NO, and N_2O molecules; and to reveal the effect of photoactivation on the particular steps of a TiO_2 reduction–oxidation cycle.

EXPERIMENTAL

A set of the following complementary techniques was used in this study: mass spectrometry, temperature-programmed desorption (TPD), diffuse-reflectance spectroscopy in the region 0.50–3.50 eV (350–2500 nm), and UV photoelectron spectroscopy (UPS). The reaction kinetics in the gas phase were studied by mass spectrometry at pressures of ~10^{-3}–10^{-1} Torr [17, 18]. The concentration and composition of adsorbed components and the energy of their binding to the surface were determined using TPD. The nature of the active sites was studied by diffuse-reflectance spectroscopy [19, 20]. The UPS technique (8.43 eV) [21] was used for determining the spectrum of the occupied electronic states of the induced defects and their position in the band scheme with respect to the Fermi level E_F.

The pretreatment of a sample (~80 mg of Degussa P-25 TiO_2; S_{sp} = 50 m^2/g) for mass-spectrometric experiments was performed *in situ* in a reactor. The reactor was equipped with a computer-controlled linear heating system for the thermal treatment of samples and TPD measurements. A digital Pirani gage allowed us to measure pressures over the range 0.001–2.5 Torr.

0023-1584/04/4502-0189 © 2004 MAIK "Nauka / Interperiodica"

Average values of the positions of maximums ($h\nu_{max}$) and half-widths ($\Delta h\nu_{1/2}$) of Gaussians obtained by the deconvolution of spectra *3*–*5* in Fig. 1

Band	$h\nu_{max}$, eV	$\Delta h\nu_{1/2}$, eV
1	1.17 ± 0.02	0.83 ± 0.03
2	2.00 ± 0.02	0.88 ± 0.02
3	2.55 ± 0.01	0.42 ± 0.03
4	2.81 ± 0.01	0.25 ± 0.03

The sample was preheated in a flow of pure oxygen (99.99%) at 0.5 Torr and $T = 850$ K. Moreover, the sample was subjected to the following sequence of treatments before each experiment: (1) evacuation to $P = 10^{-7}$ Torr at room temperature; (2) heating to 850 K and a 40-min exposure in a vacuum at this temperature ("reduced" sample) or (2a) heating at 850 K for 30 min in oxygen at 0.3 Torr with continuous mass-spectrometric monitoring of the purity of oxygen over the sample (the purity of oxygen at the reactor outlet was no lower than 99.9%) followed by a decrease in the temperature and evacuation to 10^{-7} Torr at 500 K ("oxidized" sample); and (3) cooling the sample to room temperature with evacuation. The temperature conditions of sample treatment for optical and UPS experiments were somewhat different from the above, and they will be specified below in the description of the corresponding experiments. A comparative characterization of the states of the samples was performed using the TPD spectra of adsorbed oxygen. The sample was characterized more fully using optical spectroscopy, UPS, and TPD.

Optical measurements. The experimental setup for the *in situ* studies was based on a Beckman UV 5270 spectrophotometer [19, 20]. A sample was applied to the walls of a quartz reactor and treated as described above. The diffuse-reflectance spectra ($\rho(\lambda)$) were measured over the range 2500–350 nm (0.50–3.50 eV) at 295 K before ($\rho_1(\lambda)$) and after ($\rho_2(\lambda)$) the corresponding treatment (annealing, gas adsorption, and irradiation). Here, $\rho(\lambda)$ refers to the reflectance of the sample at wavelength λ with reference to a $BaSO_4$ standard sample. In this spectral region (beyond the intrinsic absorption edge), a decrease in the value of $\rho(\lambda)$ corresponds to an increase in the absorption and vice versa. The difference spectra $\Delta\rho(h\nu) = \rho_1(h\nu) - \rho_2(h\nu)$ were analyzed; in this case, $\Delta\rho(h\nu) > 0$ corresponds to the absorption produced by the treatment. The temperature functions $d(\Delta\rho_\lambda)/dT$ were also analyzed on the linear heating of the samples; this allowed us to compare them with the TPD spectra [19, 20].

Mass-spectrometric measurements. The setup for mass-spectrometric measurements in the course of kinetic and TPD studies and experimental procedures were described previously [17, 18]. An MI-1201 automated mass spectrometer allowed us to scan up to 11 selected mass peaks within the range 12–100 amu in 13 s. The experimental results were corrected for gas sampling for analysis; this correction was no higher than 5% of the measured value at a reactor pressure of 0.05 Torr or no higher than 0.5% at $P > 0.5$ Torr. High-purity O_2, NO, and N_2O gases (99.9%) were used; nitrogen monoxide was enriched in the ^{15}N isotope by 94.9%. A DRT-120 high-pressure mercury lamp with water and band light filters was used to sample irradiation.

UV photoelectron spectroscopy (8.43 eV). The photoelectron spectrometer specialized for the *in situ* studies of extremely low concentrations of electron levels in the forbidden gap was described elsewhere [21]. The spectrometer chamber had a minimum volume (<500 cm^3) and allowed us to perform all of the required procedures *in situ* (filling with a gas, gas photoadsorption and photodesorption, photocatalytic reactions, and measurements of the TPD spectra).

RESULTS AND DISCUSSION

Induced color centers and O_2, NO, and N_2O adsorption on them. The diffuse-reflectance spectra of the TiO_2 samples treated as described above remained unchanged upon heating the samples in a vacuum or in oxygen (0.1 Torr) up to $T \le 850$ K. A measurable effect was reached by heating in a reducing atmosphere (CO or H_2; $P = 0.1$ Torr) at $T > 700$ K followed by evacuation at the heating temperature. Figure 1 (curve *2*) illustrates a typical result of this treatment as the difference between the diffuse-reflectance spectra measured before and after the treatment.

The reflectance spectra of a reduced sample were measured at room and elevated temperatures. In the region $1.50 \le h\nu \le 3.50$ eV, the reflectance remained unchanged as the temperature was varied from 300 to 850 K. However, in the region $h\nu \le 1.50$ eV, the absorption reversibly increased with temperature. Thus, at 450 K, its increase was as high as ~13%. The temperature dependence of absorption in the region $h\nu \le 1.50$ eV allowed us to attribute this absorption to free electrons, whose concentration increased on heating because of the thermal ionization of shallow donors.

The adsorption of O_2, NO, and N_2O irreversibly (with respect to gas evacuation) decreased the absorption of the reduced sample. Figure 1 (curves *3*–*5*) demonstrates the effect of treatment with O_2, NO, or N_2O at 3×10^{-2} Torr followed by evacuation on the absorption spectra of a freshly reduced sample. It can be seen that a decrease in the absorption was more significant in the low-energy region of the spectrum.

An analysis showed that curves *2*–*5* in Fig. 1 can be represented as the sum of four Gaussians (Fig. 2), whose parameters are summarized in the table. The

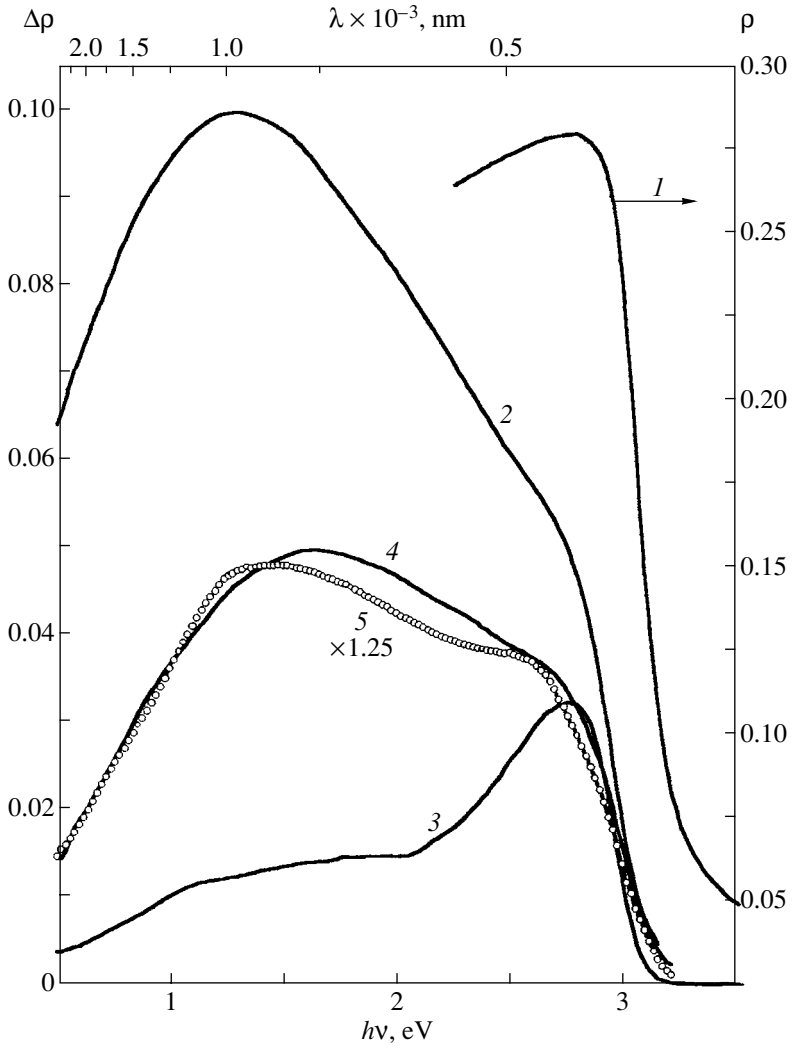

Fig. 1. (*1*) Initial diffuse-reflectance spectrum of a thin layer of Degussa P-25 TiO_2 and absorption spectra (*2*) after reduction in CO or H_2 at 800 K and the subsequent treatment in (*3*) O_2, (*4*) NO, or (*5*) N_2O at 290 K and $P = 3 \times 10^{-2}$ Torr for (*3*) ≥5 or (*4*, *5*) ≥10 min.

number and parameters of individual bands are chosen based on an analysis of the evolution of experimental spectra. Curve *7* (Fig. 2a) corresponds to the contribution of free-electron absorption to the initial spectrum. This absorption completely disappeared upon the adsorption of O_2, NO, and N_2O. Bands with maximums at 2.55 and 2.80 eV appeared in the spectrum shown in Fig. 1 (curve *3*), and they are main bands in the absorption of TiO_2 reduced with a number of polymer molecules [22]. The absorption spectrum in the region $h\nu <$ 2.50 eV should be described by at least two Gaussians because its maximum shifted from 1.25 (Fig. 1, curve *2*) to 1.90–2.00 eV (Fig. 1, curve *3*). On this basis, the total spectrum after subtracting the absorption due to free-electron absorption was resolved into four Gaussians. Figure 2 illustrates the deconvolution of the spectra of a reduced sample before and after O_2 adsorption. Thus, the minimum number of bands sufficient for describing the experimental curve was used.

Color centers (table, bands 1–4) differed in the kinetics of bleaching with oxygen at room temperature (Fig. 3). For all of the centers, the kinetic curves of bleaching were approximated to within the experimental error by a biexponential function with the characteristic times τ_1 and τ_2 of fast and slow steps, respectively. At $P = 5 \times 10^{-2}$ Torr, τ_1 = 5–10 s, whereas τ_1 = 55–85 s at $P = 5 \times 10^{-5}$ Torr (Fig. 3, curves *3′* and *4′*). At the fast step, the absorption at 0.55 eV disappeared almost completely (by 95%); the intensity of the bands at 2.00 and 1.17 eV decreased by ~70%, whereas the intensity of the bands at 2.81 and 2.55 eV decreased by ~20%. At the second step, the intensity of the bands at 2.00 and 1.17 eV decreased by 85–90%, whereas the intensity of the bands at 2.81 and 2.55 eV decreased by ~35%. Thus, the adsorption of oxygen discriminates color centers in accordance with their reactivity. The biexponential shape of the intensity decay kinetic curves for both groups of bands can be indicative of the coexistence of

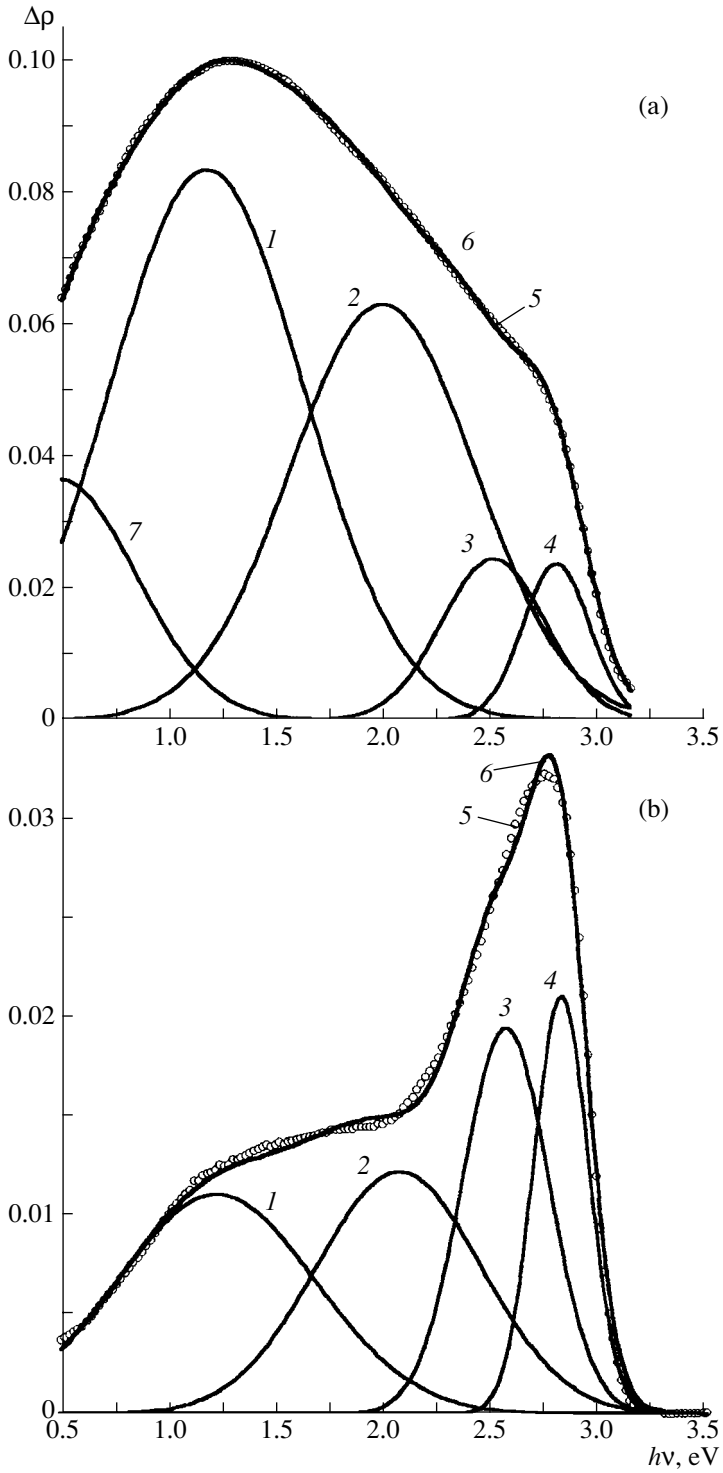

Fig. 2. Deconvolution into (*1–4*) Gaussians of the absorption spectra of reduced TiO_2: (a) before and (b) after O_2 adsorption. (*5*) Experimental absorption spectrum and (*6*) its simulation by a sum of Gaussians; (*7*) contribution of free-electron absorption to the initial spectrum.

various channels for the disappearance of the color centers. They can be related to both molecular and dissociative oxygen adsorption, which can be complicated by diffusion. The nonlinear dependence of τ_1 on pressure as P was changed from 5×10^{-2} to 5×10^{-5} Torr (curves *3* and *3*'; *4* and *4*') implies that the color centers interact with molecules through intermediate adsorption complexes rather than via a collision mechanism.

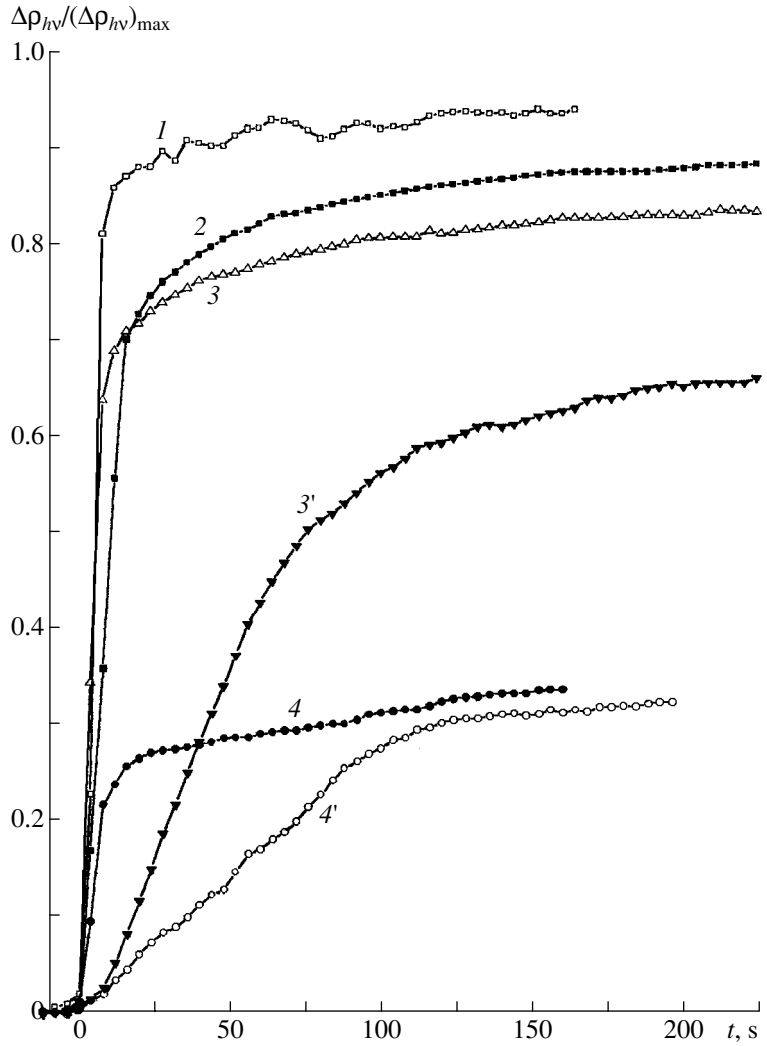

Fig. 3. Kinetics of bleaching of reduced TiO_2 on O_2 adsorption at P = (*1*–*4*) 5×10^{-2} and (*3*', *4*') 5×10^{-5} Torr; $t = 0$ corresponds to the point in time at which oxygen was added. $h\nu$ = (*1*) 0.52, (*2*) 0.92, (*3*, *3*') 1.77, and (*4*, *4*') 2.67 eV.

Henderson *et al.* [23] assumed the occurrence of these complexes in reduced rutile.

The bands at 1.17 and 2.00 eV were almost completely suppressed by oxygen adsorption even at 290 K, whereas additional thermal activation was required for the complete disappearance of the bands at 2.55 and 2.81 eV. The thermally activated annealing was accompanied by the release of oxygen. On linear heating, the annealing curve of a band at 2.80 eV and the TPD spectrum of O_2 were practically coincident; their maximums corresponded to 410 K at the heating rate β = 0.3 K/s. On the assumption that the TPD peak at 410 K is due to the discharging of the O_2^- radical anion, we concluded that both of the processes have a common step of discharging surface states [19].

The nature of the color centers in TiO_2 is the subject of wide discussion. Absorption in a wide region of 0.10–3.00 eV with a maximum at 1.00 eV, which is analogous to that shown in Fig. 1 (curve *2*), was found previously in reduced rutile [24–26]. At a low degree of reduction, the absorption maximum shifted to 0.75 eV [26]. Bands at 0.75 and 1.18 eV were attributed to oxygen vacancies that trapped two or one electron, respectively [26]. This interpretation remains the most popular although it is debatable.

The band at ~2.0 eV was detected in colloidal TiO_2 on pulsed UV irradiation [14, 15], and it was attributed to Ti^{3+} ions. Note that the band at 1.80 eV, which was attributed to *d*–*d* transitions in Ti^{3+}, was observed in the absorption spectra of organometallic compounds containing a TiO_2 structural group [27]. A peak at 1.9 eV in the electron energy-loss spectrum was related to *d*–*d* transitions in Ti^{3+} in a single crystal of rutile [28].

Kuznetsov and Krutitskaya [19] related the bands at 2.81 and 2.55 eV (see the table) to oxygen vacancies. The absorption of reduced dispersed TiO_2 in the region 2.2–3.0 eV with a maximum at ~2.9 eV, which was sta-

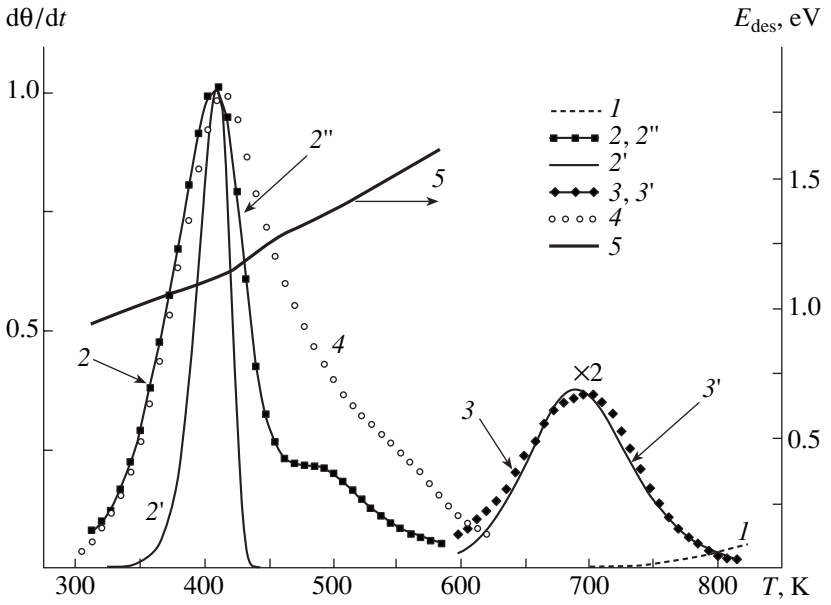

Fig. 4. TPD spectra (β = 0.2 K/s) of O_2 from the surface of TiO_2 after (*1*) heating in a vacuum at 850 K, (*2*) treatment of a reduced sample in O_2 at 290 K, (*3*) reoxidation in O_2 at 500–650 K, and (*4*) UV irradiation in O_2. Spectra *2* and *4* were normalized to the maximums; curve *2*' shows a calculated first-order peak with the parameters $\nu = 1 \times 10^{13}$ s^{-1}, E_{des} = 1.19 eV, and β = 0.2 K/s; curve *2*" shows the TPD spectrum calculated according to the model of a heterogeneous surface [17] ($\nu = 1 \times 10^{13}$ s^{-1}, β = 0.2 K/s); and curve *3*' shows a calculated second-order peak with the parameters ν = 3 cm^2/s, β = 0.2 K/s, E_{des}= 1.42 eV, and initial coverage of 1×10^8 cm^{-2}. Curve *5* shows the calculated values of E_{des}.

ble in air at room temperature, was also ascribed to oxygen vacancies [11]. Data obtained by Kurtz *et al.* [29] provide support for this stability of a portion of the defects in reduced TiO_2. The absorption band at 2.9–3.0 eV with a halfwidth of ~0.6 eV in the single crystals of TiO_2 was attributed to oxygen vacancies [30].

Thus, based on the experimental results and published data, the total absorption of reduced TiO_2 can be related to the formation of free electrons (a continuum at $h\nu \le 1.50$ eV), Ti^{3+} ions (a band at 2.00 eV), and oxygen vacancies (bands at 1.17, 2.55, and 2.81 eV). Recent calculations [31] demonstrated that oxygen vacancies in TiO_2 can form three types of centers: F^{2+} (without electron capture), F^+ (with one electron), and F (with two electrons). Electron levels in the forbidden gap 0.20, 1.78, and 0.87 eV below the bottom of the conduction band correspond respectively to these centers. By this it is meant that the levels of F and F^+ centers at room temperature are occupied by electrons and can be color centers. Thus, a decrease in the intensities of a continuum at $h\nu \le 1.50$ eV and bands at 1.17 and 2.00 eV in the course of oxygen adsorption at room temperature was due to the capture of electrons from the conduction band, as well as from Ti^{3+} local levels, F, and/or F^+centers.

A specific feature of the bands at 2.55 and 2.81 eV is that an additional thermal activation is required for their complete disappearance. This suggests the coexistence of two types of centers. Centers of the first type are arranged on the surface and they were suppressed at the initial step at room temperature. It is likely that centers of the second type occur in a subsurface layer, and the reaction of oxygen with them requires an additional activation. The bleaching of bands at 2.55 and 2.81 eV at $T \approx 400$ K can occur via two channels: (1) the recharging of color centers with electrons, which became free on the decomposition of O_2^- complexes and (2) the filling of oxygen vacancies with atomic oxygen generated in the course of O_2^- decomposition [19]. The surface activity of TiO_2 toward isotope exchange at $T > 400$ K is indicative of the possibility of the appearance of atomic oxygen [32, 33].

Analysis of adsorbed oxygen species by the TPD method. The irradiation of both oxidized and reduced samples in a vacuum resulted in the photodesorption of oxygen and in the appearance of color in the sample [1]. However, we observed the photoadsorption of oxygen on irradiation. The effect was detected by mass spectrometry as a decrease in the reactor pressure followed by the TPD analysis of an adsorbed phase. Figure 4 (curve *2*) demonstrates a typical TPD spectrum of oxygen adsorbed in control experiments with an unirradiated reduced sample. After the oxidation of the sample, the TPD spectrum exhibited a new peak at 700 K (Fig. 4, curve *3*); however, the total adsorption capacity of the sample decreased by more than one order of magnitude. The main peak at 410 K, which is typical of

reduced TiO_2, was related to the O_2^- radical anion adsorption species [23]. Its intensity can be used for evaluating the degree of sample reduction.

Figure 4 (curve *4*) demonstrates the TPD spectrum of photoadsorbed oxygen. In addition to an increase in the intensity of the peak at 410 K, the contribution of the region of 450–600 K to the total spectrum considerably increased. A characteristic feature of this adsorption species is its high activity in oxidation and isotope-exchange reactions [32–34]. The atomic structure of this species remains questionable. Desorption in this temperature range is related to the degradation of $[O_S^- \ldots O_2]$ complexes (the subscript "S" refers to surface oxide centers) formed by the interaction of O_2 with the photogenerated hole centers of wide-gap oxides [34]. At the same time, Epling *et al.* [35] detected an atomic adsorption oxygen species on a reduced single crystal of rutile; the concentration of this species noticeably decreased at $T > 500$ K. A peak at 700 K (Fig. 4, curve *3*) is likely due to associative desorption from atomic adsorption species [36]. Thus, the types of O_2 adsorption typical of wide-gap oxides manifested themselves on TiO_2 [34].

Figure 4 illustrates the results of the simulation of experimental spectra using the Polani–Wigner equation

$$-d\theta/dt = \nu(\theta^n/\beta)\exp(-E_{des}/(RT)),$$

where θ is the coverage, ν is the frequency factor, and n is the order of desorption ($n = 1$ or 2 for molecular or associative desorption, respectively). The parameters were chosen based on the coincidence of maximums in the experimental and calculated curves. It can be seen (Fig. 4, curve *2*) that the entire TPD spectrum cannot be described using constant values of n, ν, and E_{des}. We used the model of a nonuniform surface, which was tested previously [17]. In this model, the quantity E_{des} is approximated with the following polynomial function of coverage:

$$E_{des}(\theta_i) = \sum_{k=1}^{K} \alpha_k (1-\theta)^{k-1},$$

where α_k are polynomial coefficients, k is the exponent, and i is the point number of the TPD spectrum. On the assumption that ν and n are constant, equations for each of the N points of the TPD spectrum can be written. The coverage θ_i is defined as

$$\theta_i = 1 - \int_{T_0}^{T_i} \frac{d\theta_i}{dT} dT.$$

The set of $(K + 1)$ equations is solved numerically by the least-squares technique; this allows us to determine the values of α_k, ν, and n. The degree of polynomial K is chosen from the best approximation to the experimental results.

Figure 4 (curve *2*") demonstrates the result of the simulation. The model adequately describes the result obtained: the simulation error is no higher than the measurement error. Adsorption complexes are nonuniform in terms of the strength of binding to the surface. The value of E_{des} (Fig. 4, curve *5*) varied from 0.95 to 1.60 eV. It was no higher than 1.12 eV for 50% and 1.37 eV for 90% oxygen complexes. The energetic heterogeneity can be fully explained by the above variety of adsorption sites.

Reactions of N_2O and NO with a reduced surface. The addition of N_2O to a reduced sample was accompanied by the appearance of disproportionation products (N_2 and NO) in the gas phase. In this case, the balance of oxygen in the gas phase was disturbed: a portion of the oxygen remained on the sample. Shultz *et al.* [37] found that oxygen vacancies were filled as a result of N_2O decomposition, and the dioxide surface became near-stoichiometric.

The irradiation of the N_2O/TiO_2 system resulted in an increase in both the pressure of N_2 and N_2O and the ratio NO : N_2O. This suggests the coexistence of two photoactivated processes: N_2O photodesorption and disproportionation. Rusu and Yates [9] studied the photodecomposition of N_2O on TiO_2 at 157 K, and they did not detect the appearance of NO in a gas or adsorbed phase. This is likely due to a difference between the reaction paths at 293 and 157 K. In particular, with the use of TPD, we found that a low-temperature N_2O adsorption species is desorbed at room temperature, and this species does not participate in the reaction at 293 K.

On the addition of NO to a reduced sample, N_2 and N_2O were released into the gas phase. Irradiation resulted in the photoadsorption of NO and in an increase in the rates of release of the disproportionation products (N_2 and N_2O) into the gas phase.

At extremely low coverages (~10^{-6} monolayer), the TPD spectrum exhibited two peaks with maximum temperatures of 380 and 460 K, which merged into a broad peak with a maximum at 430–440 K as the coverage was increased (Fig. 5, curve *1*). The occurrence of two NO adsorption species was also supported by the appearance of two bands at 1925 and 1910 cm^{-1} in the IR spectrum [38]. Moreover, a band at 2240 cm^{-1} appeared, which was attributed to the ν_3-vibration mode of N_2O [38]. As compared with dark adsorption, the TPD spectra of photoadsorbed NO exhibited an additional peak of NO at 330 K, high-temperature peaks of O_2 and NO at 700 K (Fig. 5, curves *3*, *4*), and a peak of N_2O (not shown in Fig. 5). As mentioned above, the O_2 peak shape is typical of associative desorption, whereas the peak intensity correlates with the degree of sample reduction, that is, with the amount of oxygen vacancies. This fact together with the estab-

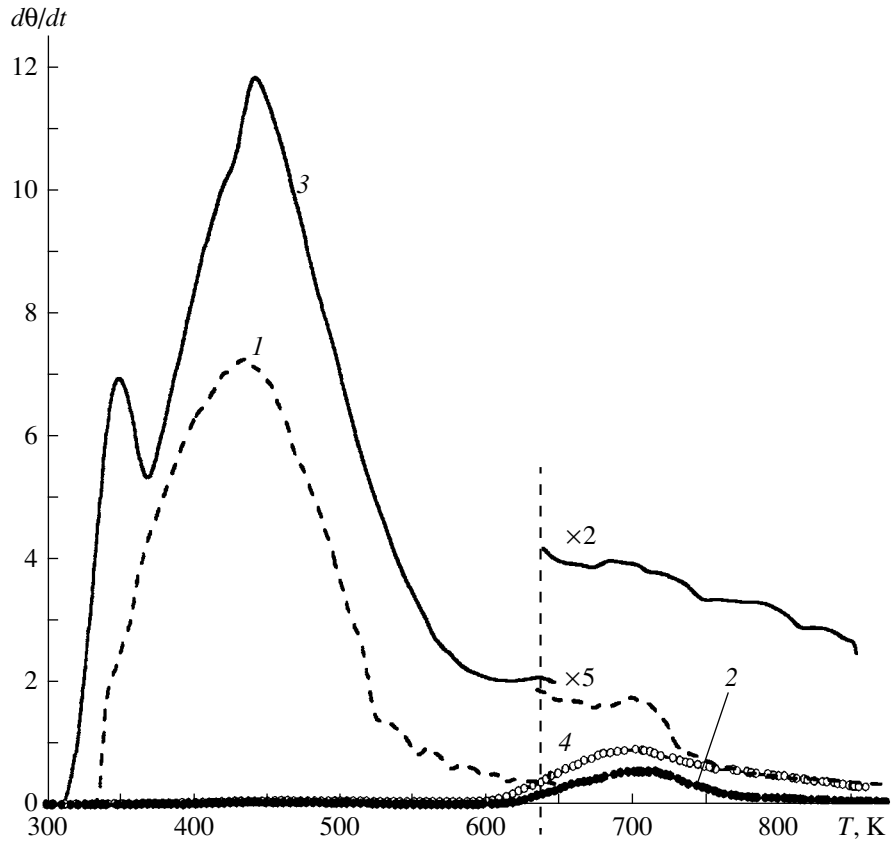

Fig. 5. TPD spectra of (*1*, *3*) NO and (*2*, *4*) O_2 after the (*1*, *2*) dark adsorption and (*3*, *4*) photoadsorption of NO on TiO_2.

lished facts of N_2 and N_2O release and the bleaching of oxygen vacancies on NO adsorption can be explained by the formation of atomic oxygen and by filling the oxygen vacancies with this oxygen.

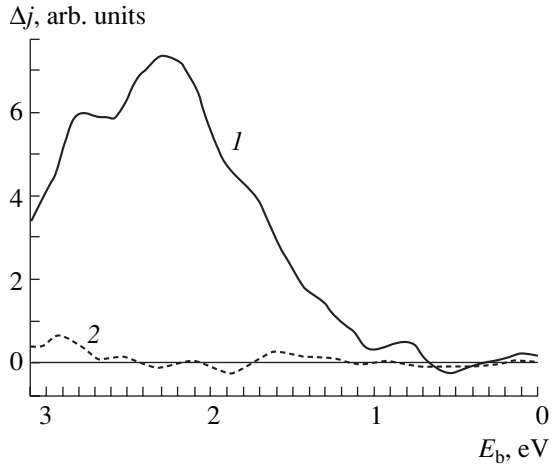

Fig. 6. Changes in the density of the occupied states (Δj) of TiO_2 in the near-Fermi region according to UPS data as a result of (*1*) heating to 723 K in an ultrahigh vacuum and (*2*) the subsequent treatment in O_2 at P = 0.1 Torr for 30 min. The binding energy is measured from the Fermi level.

UPS. Compared to diffuse-reflectance spectroscopy, UPS detects changes in the spectrum of occupied electronic states at earlier stages of reduction. Thus, local states in the forbidden gap up to the level E_b = 0.7 eV were reliably detected after heating in an ultrahigh vacuum at 723 K (Fig. 6, curve *1*). These states are due to the appearance of intrinsic defects. As can be seen in Fig. 6, the density of states increased in the course of heating over the entire region and exhibited maximums at 2.4 and 2.8 eV. The results of optical and UPS measurements are consistent (within the limits of measurement and simulation errors) as the Fermi level lies 0.15 eV below the bottom of the conduction band and optical absorption maximums at 2.55 and 2.81 eV are due to electron transitions from local states to the bottom of the conduction band.

The subsequent addition of oxygen to the sample dramatically decreased the density of the occupied states over the entire region of 0.7–3.1 eV (Fig. 6, curve *2*). The sample recovered to its original state (Fig. 6, curve *1*) upon heating to 723 K in an ultrahigh vacuum; in the course of this heating, the desorption of oxygen was detected by mass spectrometry. Note that local states almost completely disappeared from photoelectron spectra upon oxygen adsorption at room temperature, whereas bands at 2.55 and 2.81 eV partially remained in optical spectra. This discrepancy can be reasonably

explained in terms of the model proposed for the formation of surface and subsurface defects. The photoelectron spectra were obtained in samples with a low degree of reduction, which affected only the surface, whereas the reduction in optical measurements also affected a near-surface region of the sample. Therefore, in the former case, near-surface defects, the bleaching of which requires an additional thermal activation (see above), were absent.

Thus, this work is an initial stage in studying the applicability of intrinsic structural defects to the sensitization of TiO_2-based photocatalysts to the region of nonintrinsic absorption with $\lambda \geq 400$ nm.

ACKNOWLEDGMENTS

This study was supported in part by the Federal Special Scientific and Technical Program "Research and Development Work in Priority Branches of Science for 2002–2006," Condensed Media Section.

REFERENCES

1. Formenti, M., Courbon, H., Juillet, F., Lissatchenko, A., Martin, J.R., Meriaudeau, P., and Teichner, S.J., *J. Vac. Sci. Technol.*, 1972, vol. 9, no. 2, p. 947.
2. Disdier, J., Herrmann, J.-M., and Pichat, P., *J. Chem. Soc., Faraday Trans. I*, 1983, vol. 79, p. 691.
3. Linsebigler, A., Lu, G., and Yates, J.T., Jr., *Chem. Rev.*, 1995, vol. 95, no. 3, p. 735.
4. Ghosh, F.R. and Maruska, H.P., *J. Electrochem. Soc.*, 1977, vol. 124, p. 1516.
5. Anpo, M., *Stud. Surf. Sci. Catal.*, 2000, vol. 130, p. 157.
6. Sato, S., *Chem. Phys. Lett.*, 1986, vol. 123, nos. 1–2, p. 126.
7. Diebold, U., *Surf. Sci. Rep.*, 2003, vol. 48, nos. 5–8, p. 53.
8. Linsebigler, A., Lu, G., and Yates, J.T., Jr., *J. Phys. Chem.*, 1996, vol. 100, p. 6631.
9. Rusu, C.N. and Yates, J.T., Jr., *J. Phys. Chem. B*, 2001, vol. 105, no. 13, p. 2596.
10. Ichicashi, Y., Yamashita, H., Souma, Y., Zhang, S.G., Anpo, M., Matsumura, Y., and Tatsumi, T., *Appl. Sufr. Sci.*, 1997, vols. 121/122, p. 305.
11. Nakamura, I., Negishi, N., Kutsuna, S., Ihara, T., Sugihara, S., and Takeuchi, K., *J. Mol. Catal., A: Chem.*, 2000, vol. 161, p. 205.
12. Serpone, N. and Lawless, D., *Langmuir*, 1994, vol. 10, p. 643.
13. Nikisha, V.V., Shelimov, B.N., and Kazanskii, V.B., *Kinet. Katal.*, 1971, vol. 13, no. 3, p. 774.
14. Bahnemann, D., Henglein, A., and Spanhel, L., *Farad. Discuss. Chem. Soc.*, 1984, no. 78, p. 151.
15. Rothenberger, G., Moser, J., Gratsel, M., Serpone, N., and Sharma, D.K., *J. Am. Chem. Soc.*, 1985, vol. 107, no. 26, p. 8054.
16. Sorescu, D.C. and Yates, J.T., Jr., *J. Phys. Chem. B*, 2002, vol. 106, p. 6184.
17. Lisachenko, A.A., Chikhachev, K.S., Zakharov, M.N., Basov, L.L., Shelimov, B.N., Subbotina, I.R., Che, M., and Coluccia, S., *Top. Catal.*, 2002, vol. 20, nos. 1–4, p. 119.
18. Kuznetsov, V.N. and Lisachenko, A.A., *Kinet. Katal.*, 1986, vol. 31, no. 3, p. 659.
19. Kuznetsov, V.N. and Krutitskaya, T.K., *Kinet. Katal.*, 1996, vol. 37, no. 3, p. 472.
20. Kuznetsov, V.N. and Lisachenko, A.A., *Zh. Prikl. Spektrosk.*, 1991, vol. 54, no. 2, p. 272.
21. Lisachenko, A.A. and Aprelev, A.M., *Pis'ma Zh. Tekh. Fiz.*, 1995, vol. 21, no. 17, p. 9.
22. Kuznetsov, V.N. and Malkin, M.G., *Zh. Prikl. Spektrosk.*, 2000, vol. 67, no. 5, p. 558.
23. Henderson, M.A., Epling, W.S., Perkins, C.L., Peden, C.H.F., and Diebold, U., *J. Phys. Chem. B*, 1999, vol. 103, no. 25, p. 5328.
24. Cronemeyer, D.C., *Phys. Rev.*, 1952, vol. 52, no. 1, p. 876.
25. Breckenridge, R.G. and Hosler, W.R., *Phys. Rev.*, 1953, vol. 91, no. 4, p. 793.
26. Cronemeyer, D.C., *Phys. Rev.*, 1959, vol. 113, no. 5, p. 1222.
27. Jeske, P., Haselhorst, G., Weyhermuller, T., Wieghardt, K., and Nuber, B., *Inorg. Chem.*, 1994, vol. 33, no. 11, p. 2462.
28. Henrich, V.E., Dresselhaus, G., and Zeiger, H.J., *Phys. Rev. Lett.*, 1976, vol. 36, no. 22, p. 1335.
29. Kurtz, R.L., Stockbauer, R., Madey, T.E., Roman, E., and de Segovia, J.L., *Surf. Sci.*, 1989, vol. 218, no. 1, p. 178.
30. Sekiya, T., Ichimura, K., Igarashi, M., and Kurita, S., *J. Phys. Chem. Solids*, 2000, vol. 61, p. 1237.
31. Chen, J., Lin, L.-B., and Jing, F.Q., *J. Phys. Chem. Solids*, 2001, vol. 62, p. 1257.
32. Beck, D.D., White, J.M., and Ratcliffe, C.T., *J. Phys. Chem.*, 1986, vol. 90, no. 14, p. 3132.
33. Yanagisaw, Y. and Ota, Y., *Surf. Sci.*, 1991, vol. 254, nos. 1–3, p. 433.
34. Lisachenko, A.A., *Phys. Low-Dim. Struct.*, 2000, vols. 7/8, p. 1.
35. Epling, W.S., Peden, C.H.F., Henderson, M.A., and Diebold, U., *Surf. Sci.*, 1998, vols. 412/413, p. 333.
36. Kuznetsov, V.N., *Kinet. Katal.*, 2002, vol. 43, no. 3, p. 934.
37. Shultz, A.N., Hetherington, W.M., Baer, D.R., Wang, L.-Q., and Engelhard, M.H., *Surf. Sci.*, 1997, vol. 392, p. 1.
38. Gerasimov, S.F., *Cand. Sci. (Phys.–Math.) Dissertation*, Leningrad: Leningrad. Gos. Univ., 1986.